Mathematics in Applied Sciences and Engineering
Online First, pp.**1-11**

https://ojs.lib.uwo.ca/mase
https://doi.org/10.5206/mase/15477

FISHER INFORMATION APPROACH TO UNDERSTAND THE GOMPERTZ MODEL

AVAN AL-SAFFAR AND EUN-JIN KIM

Abstract. As a measure of sustainability, Fisher information is employed in the Gompertz growth model. This article examines the gompertz growth equation which describes the time evolution of large-scale variables such as the human body, with control parameters incorporating the effect of therapies on small-scale variables. Control parameters are typically assumed to be constants, but in reality, they may be subject to fluctuations. The effect of different oscillatory modulations is examined on the system's evolution and Probability Density Function (PDF). For a sufficiently large frequency of periodic fluctuations occurring in both positive and negative feedbacks, the system maintains its initial conditions. A similar PDF is shown regardless of the initial values when there are periodic fluctuations in positive feedback. By periodic fluctuations in negative feedback, the Gompertz model can lose its self-organization. Finally, despite the fact that the Gompertz and logistic systems evolve differently over time, the results show that they are exceptionally similar in terms of information and sustainability.

1. Introduction

The Gompertz model has been evoked as a growth curve by numerous researchers for both biological and economic phenomena. Specifically, the Gompertz model (1.1) was employed significantly in different areas, in order to demonstrate population dynamics and to track their properties such as: specifying a mortality law in actuarial science, tumor growth and suppression modeling in medicine, depicting the outgrowth of organisms in biology, in ecology, etc. (see [12], [4] and references there in). In common, the Gompertz model is written as follows:

$$x(t) = e^{a(1-e^{-bt})}, \tag{1.1}$$

where a and b are positive quantities [4, 15, 17]. From Eq. (1.1), x approaches zero when t display a tendency towards negative infinity; whereas x gets close to the equilibrium point $x^* = e^a$ as t tends towards positive infinity, which is asymptotically stable and attracts all the initial states [10]. Eq. (1.1) presents a sigmoidal curve for $x(t)$ and can model human's height and mass, a fish community, a rabbit (see [18], [14] and references therein), diverse malicious tumors [7, 8]. In particular, the Gompertz equation was successfully fitted to data of tumor growth for the first time in the 1960s by Laird [7], where tumors are cellular populations increasing in a restricted space with a limited availability of nutrients. Furthermore, Waliszewski [15] showed that the derivative of the Gompertz function is a PDF, and the probability distribution of it is a solution of non-Gaussian form. The Verhulst, Richards, Comperzt, and modified Malthus model were used to to understand the dynamics of water volume growth in a reservoirs [5].

Received by the editors 2 November 2022; accepted 14 December 2022; published online 26 December 2022.
2010 *Mathematics Subject Classification.* Primary 54C40, 14E20; Secondary 46E25, 20C20.
Key words and phrases. Dynamical system, sustainability, fisher Information, periodic fluctuations, probability density function, equilibrium points.

A periodic Gompertz model with stochastic impulsive coefficients is investigated by Wang and Liu [16]. A modulation in the model parameters is studied using Fisher information. Fisher Information indexes for dynamic systems in periodic steady states were developed and applied to a simple two-species Lotka-Volterra predator-prey model [9]. Further comparison is conducted based on changes in information during growth between the Logistic growth model and Gompertz growth model [13]. In order to achieve regime change, an ecological system must be able to change its properties to a great extent [6].
The purpose of this article is to study the effects of oscillatory modulations on the parameters and examine sustainability by using Fisher information. Also, the similarity and differences between the Gompertz model and the logistic function of growth are presented. The reminder of the article is organized as follows. Section §2 introduces the model. In section §3, the Gompertz model with fluctuations in both terms is presented, and present PDFs, Fisher information. Also, it is compared with the logistic model. In sections §4 and §5, we summarize the results for a periodic modulation of the model parameters in the negative feedback or positive feedback, respectively. Conclusions are provided in section §6.

2. The model

The model is given by:

$$\frac{dx}{dt} = cx - bx\log x. \tag{2.1}$$

Where, c and b are experimental coefficients specifying the curve's slope (e.g [15] and references there in); c is the rate of population growth, and b is the average of population death, t is time, x is the population of any type, and $x_0 = x(t=0)$ is the population initial size. Eq.(2.1) presents a population asymptotically reaching the maximum value $x^* = e^{(c/b)}$ which is the stable equilibrium point. The first term cx (linear) with $c > 0$ represents positive feedback whereas the second term $bx\log(x)$ (nonlinear) with b¿0 represents negative feedback.
In the case of a periodic fluctuation $D_0\sin(\omega t)$, is included in the different model parameters, where D_0 and ω are the amplitude and frequency of the modulation, respectively. As in the Logistic equation in [1], the value of the amplitude is fixed to be $D_0 = 7$, to explore the influence of different values of ω and x_0 on the response of the Gompertz model.
Specifically, it may be beneficial to study three different cases of the Gompertz model. Each case will be presented individually in the next sections III-V. Numerical simulations and analytical analyses are performed.

Case-1: $\frac{dx}{dt} = [D_0\sin(\omega t)]\, x\,(1-\log x)$.

Case-2: $\frac{dx}{dt} = [D_0\sin(\omega t)]\, x - b\, x\log x$.

Case-3: $\frac{dx}{dt} = cx - [1 + D_0\sin(\omega t)]\, x\log x$.

Each case will be discussed separately in the following sections 3-5. We perform both analytical and numerical analyses.

3. Case-1: Similar Fluctuation in the Positive and Negative Feedback

The following model is considered:

$$\frac{dx}{dt} = [D_0\sin(\omega t)]\, x(1-\log x). \tag{3.1}$$

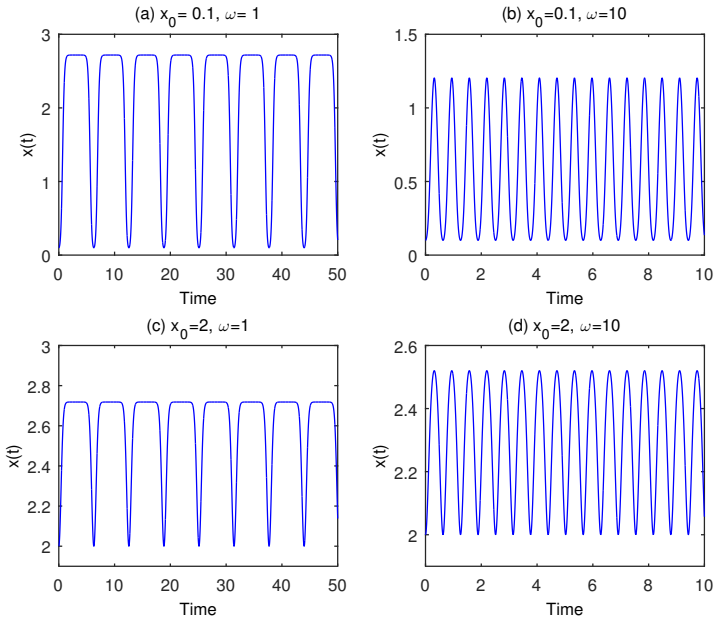

FIGURE 1. Time trace of $x(t)$ for $x_0 = 0.1, 2$ and $\omega = 1, 10$.

The analytical solution to Eq. (3.1) can be found in the following form:

$$x(t) = e^{\left(1-\left[\left(1-\log(x_0)\right)\, e^{\left\{-\frac{D_0}{\omega}\left(1-cos(\omega t)\right)\right\}}\right]\right)}, \tag{3.2}$$

where x_0 is the initial value of x at $t = 0$. We show the typical time history of $x(t)$ for different values of ω and x_0 in Fig. 1.

In Fig. 1, the time trace of x for two different values of ω, $\omega = 1, 10$ and two initial values $x_0 = 0.1, 2$ are shown.

From Fig. 1, for small ω, $x(t)$ tends to reach the equilibrium point ($x^* = e$) without paying attention to the value of x_0 where the perturbation's time-scale becomes much larger than the system's response time. In contrast, for large ω, the time-scale is much shorter than the system's response time and so that x(t) preserves its initial values and on no occasion can outreach the equilibrium point (see Fig. 1). In Fig. 2, the maximum and minimum of x in blue solid line and red dashed lines, respectively against ω for different values of x_0 is presented. It is obvious that a difference between column 1 and 2 which show the results for different x_0. For $x_0 = 0.1$ the maximum value of x decreases extremely faster as ω increases than for $x_0 = 2$. In comparison, for $x_0 = 2$, $x(t)$ does not deviate from its initial conditions similar to Fig. (1) (b), (d). To show this clearly, the measure of relative variation of the maximum values of x is displayed to quantify the conservation of x_0. . This is shown in Fig. 2 (e)-(f).

We compute the ratio of the change in the maximum of x to determine the maintenance of initial conditions.

$$\frac{Initial\ value - Maximum\ of x}{Maximum\ of x}\ 100\% \tag{3.3}$$

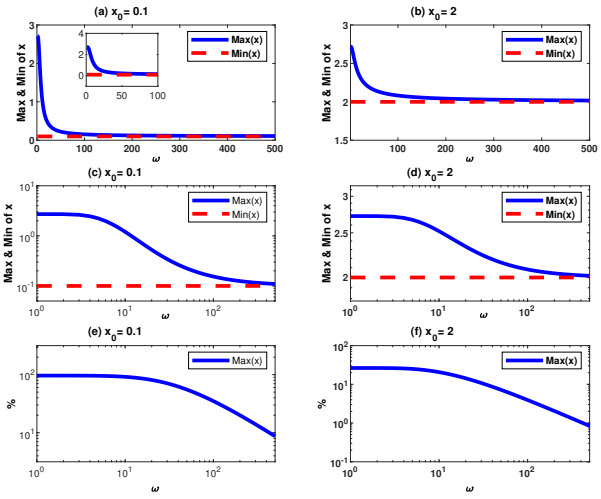

FIGURE 2. We fixed D_0 to be $D_0 = 7$, $x_0 = 0.1$ in panels (a), (c) and (e) and $x_0 = 2$ in panels (b), (d) and (f). (c), (d), (e) and (f) are shown in log-log scales.

It has been found that % is almost 100 in Fig. 2 (e)-(f) for $\omega \leq 10$. For sufficiently large $\omega \geq 10$, we observe nearly straight lines which indicates that the percentage change decreases with ω as a power-law in both cases where Panels (e) and (f) are presented in log-log scale.

3.1. **Probability Density Function.** In this section, we compute the Probability density function (PDF) of x and examine the effect of ω and x_0 on PDF. To this end, we link the time spent by the system state at x to the probability of observing the system at a particular value of x [2, 3, 11].

$$p[x]\, dx = p[t]\, dt. \tag{3.4}$$

Since t is a continuous variable with a uniform probability density:

$$p[t] = constant = A, \tag{3.5}$$

We combine Eqs. (3.4) and (3.5) and obtain a PDF of x as:

$$p[x] = p[t] \left|\frac{dt}{dx}\right| = A \left|\frac{dt}{dx}\right| = \frac{A}{u}, \tag{3.6}$$

where

$$u = \frac{dx}{dt}. \tag{3.7}$$

Now we can obtain PDF of x as follow:

$$p[x] = \frac{A}{D_0 \sin(\omega t)\; x\,(1 - \log(x))}. \tag{3.8}$$

We use Eq. (3.2) to replace $sin(\omega t)$ in Eq. (3.8) by a function which only depends on x [see Eq. (3.9)] through using the identity $\left(\sin(\omega t) = \sqrt{1 - \cos^2(\omega t)}\right)$ as follows:

$$\cos(\omega t) = 1 + \left(\frac{\omega}{D_0} \log\left[\frac{1 - \log(x)}{1 - \log(x_0)}\right]\right). \tag{3.9}$$

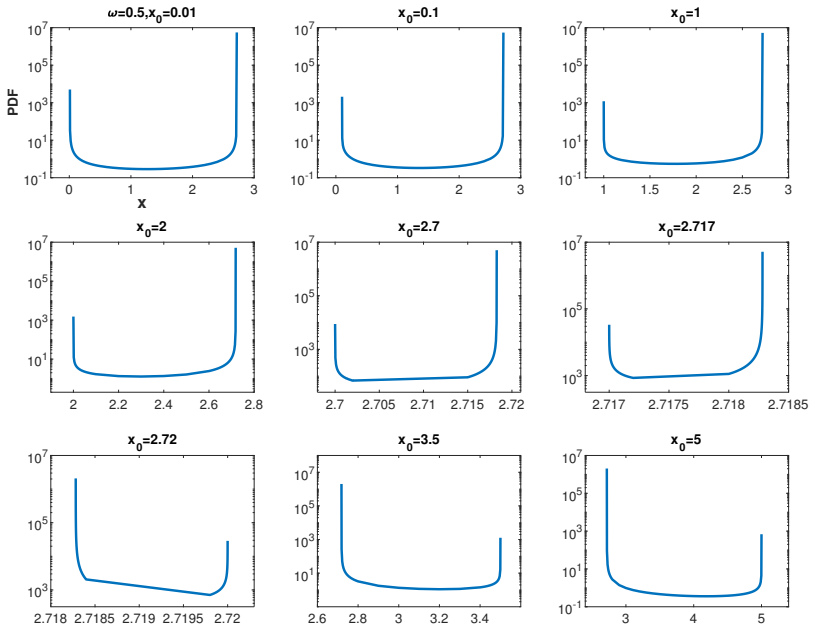

FIGURE 3. PDF of $x(t)$ for $D_0 = 7$ and $\omega = 0.5$ by using different values of x_0. All the sub-figures have the same axis labels.

It is mentioned that the PDF relies on x_0 for$\omega = 0.5$ in Fig. 3. A bimodal PDF is noticed in every case with various distance between the two ends. The first peak appears at $x = x_0$ whereas the second peak can be seen at x^*. For $x_0 < x^*$, the left peak is always lower than the right peak at equilibrium while for $x_0 > x^*$; the left peak becomes higher than the right peak as x_0 is larger than the equilibrium point.

A very identical behavior is observed for differentω (e.g., $\omega = 2$ [Figures are not shown]. For small x_0, the system exhibits a wide PDF but for large values of x_0, the PDF starts to shrink as can be seen in Fig. 1; the system can never reach the equilibrium point and maintains its initial conditions.
In the following section we will relate these findings to Fisher information.

3.2. **Fisher information.** Fisher information is utilized to study the effects of modulation in model parameters. Fisher information as a function of the system's variability is evoked to investigate whether the Gompertz function is sustainable or not (The Fisher Information changes as the system's state trajectory tracks changes in its dynamic regime). Note that a PDF biased to particular x values has higher Fisher information.
By following the results in [1], for a single measurable variable x, we find the Fisher information FI calculated from the PDF of x ($p(x,t)$) as follows:

$$FI = \int \frac{1}{p(x)} \left(\frac{dp(x)}{\partial x} \right)^2 dx. \tag{3.10}$$

Since

$$\frac{\partial p[x]}{\partial t} = -\frac{A}{u^2} \frac{du}{dt}, \tag{3.11}$$

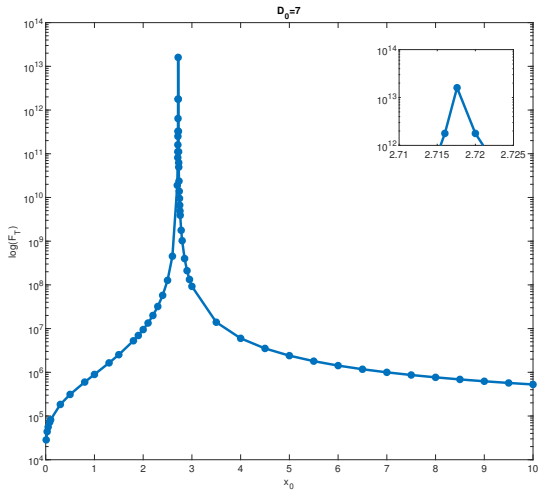

FIGURE 4. Asymptotic value of F_T against x_0 for $\omega = 0.5$. A local maximum is observed at $x_0 \simeq x^*$ where $x^* = exp(1)$

we compute the time averaged Fisher information (F_T):

$$F_T = \frac{A}{T}\int_0^T \frac{1}{(u(t))^4}\left(\frac{du}{dt}\right)^2 dt = \frac{1}{T}\int_0^T \frac{1}{A}\left(\frac{\partial p(x)}{\partial t}\right)^2 dt. \tag{3.12}$$

From Eqs. (3.1), (3.11) and (3.12), we obtain:

$$F_T = \frac{A}{T}\int_0^T \frac{[\frac{\omega\cos(\omega t)}{\sin(\omega t)} - \log(x)D_0\sin(\omega t)]^2}{[D_0\sin(\omega t)\ (x - x\log(x))]^2}\, dt. \tag{3.13}$$

F_T is the Fisher information averaged over the total time duration T; A is a normalization constant. In this section, the sustainability of our system is checked by computing F_T for different initial conditions. F_T is displayed for ($D_0 = 7$), different x_0 and $\omega = 0.5$.

In Fig. 4, fisher information is increased as x_0 increases close to $x_0 \simeq x^*$ while F_T decreases beyond $x_0 \simeq x^*$. This means that a local maximum is found at x_0 close to x^*. Also, for $x_0 > x^*$, it is observed that the curve monotonically decreases as x_0 increases because of the presence of high variability, as the system loses its functionality, thus, lower Fisher information is noticed (see Fig. 4. It is found that similar behavior for $\omega = 2$ [Figures are not shown]. In this case, the high Fisher Information indicates that the system is sustainable (less disorder), whereas the low Fisher Information indicates that the Gompertz equation is unsustainable, which means that the population cannot survive under these conditions (specific parameter values).

3.3. **Comparison with the logistic model.** The above results are compared with the logistic model governed by:

$$\frac{dx}{dt} = N_0\sin(\omega t)\, x\left(1 - \frac{x}{K}\right), \tag{3.14}$$

where N_0 and ω are amplitude and frequency of the modulation, respectively, and K is the carrying capacity of the logistic system. A PDF of x at different initial conditions in is displayed in Fig. 5.

In Fig. 5, PDF of $x(t)$ is displayed for fixed value of ω, $\omega = 0.5$ but for different initial conditions. It is observed similar results as in Fig. 3. This bimodal distribution produces from the maintenance of

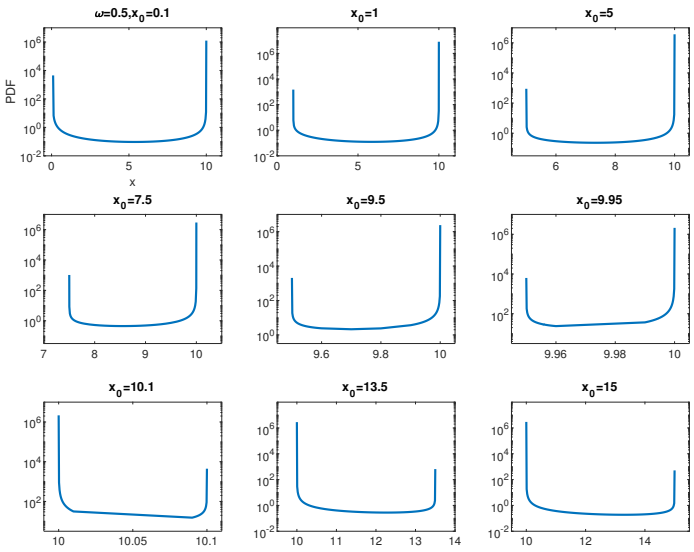

FIGURE 5. PDF for $N_0 = 5$, $K = 10$ and $\omega = 0.5$ and different values of x_0. All the sub-figures have the same axis labels.

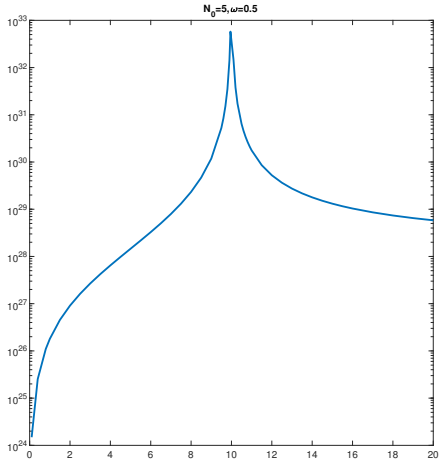

FIGURE 6. F_T for $N_0 = 5$, $K = 10$ and $\omega = 0.5$ and different x_0.

x_0 against the tendency of x approaching ($K = 10$). Analytically, it is show F_T as follows:

$$F_T = \frac{A}{T}\int_0^T \frac{\left[\frac{\omega\cos(\omega t)}{\sin(\omega t)} + \left((1-\frac{2x}{K})N_0\sin(\omega t)\right)\right]^2}{\left[N_0\sin(\omega t)\,(x-\frac{x^2}{K})\right]^2}\,dt. \tag{3.15}$$

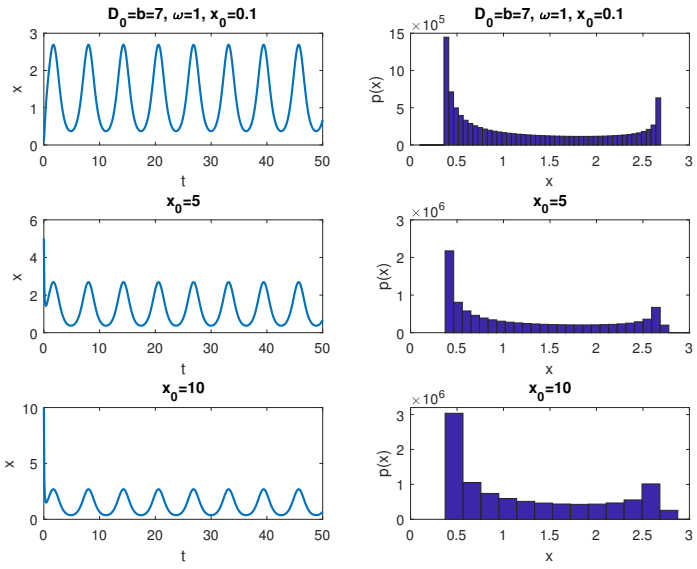

FIGURE 7. Time trace of $x(t)$ and PDF of x for different values of $x_0 = 0.1, 5, 10$ and $\omega = 1$.

F_T in Fig. 6 where it can see the maximum F_T at $x_0 \simeq x^*$ similarly to the Gompertz model. Therefore, both the Gompertz case-1 and logistic case-1 (see [9]) show less variability (more sustainability) close to the stable equilibrium point.

4. Case-2: Perturbation in the positive feedback (linear term)

A periodic modulation for the linear term is added while keeping (b=constant).

$$\frac{dx}{dt} = \Big(D_0 \sin(\omega t)\ x\Big) - b\ x \log(x), \tag{4.1}$$

where the value of b is kept constant. The analytical solution to Eq. (4.1) can be found as:

$$x = \frac{\big(D_0(b\sin(\omega t) - \omega\cos(\omega t))\big) + (D_0\omega d) + ((b^2+\omega^2) d \log(x_0))}{(b^2+\omega^2)}, \tag{4.2}$$

where

$$d = \exp(-bt).$$

By using this analytical solution, $x(t)$ is presented for different x_0 in the first column and PDF of x in the second column (see Fig. 7).

Specifically in Fig. 7, the impact of different x_0 on PDFs for $b = D_0 = 7$, $\omega = 1$ is observed. The PDFs show the same bimodal PDF for all initial conditions. Thus, case-2 reaches the same equilibrium PDF independent of x_0 similar to the results of the logistic model. That is, Fisher information F_T is also independent of x_0.

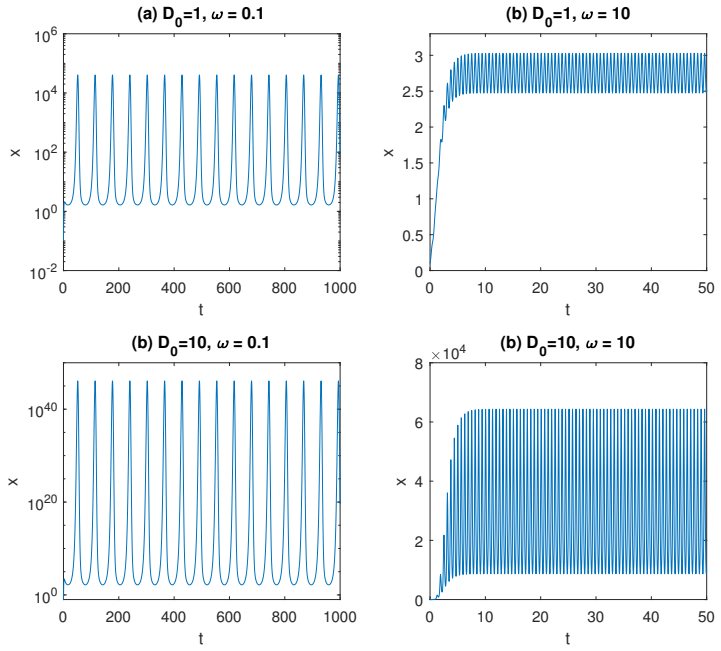

FIGURE 8. $x(t)$ against t for $D_0 = 1, 10$ and $\omega = 0.1, 10$. For all cases $x_0 = 0.1$, $B = 1$, $c = 1$.

5. Case-3: Perturbation in the negative feedback (nonlinear term)

In this case, the negative feedback contains modulation:

$$\frac{dx}{dt} = cx - (1 + D_0 \sin(\omega t))x \log(x). \tag{5.1}$$

The nonlinear term contained a periodic modulation effectively minimizes the influence of the death rate and promotes exponential growth (see Fig. (8)). For large value of D_0 and small ω in Fig. 8, it is observed that the solution grows exponentially.

In Fig. 9, PDFs for $D_0 = 0.5$ emerged in the first row and $D_0 = 1$ in the second row, respectively. For $D_0 = 1$, a bimodal PDF is noticed for all ω, the PDFs become broader as ω decrease. The intermittency burst demonstrated by the high-amplitude peaks leads to the broadening of PDFs as ω decrease.

6. Conclusions

The effects of different initial conditions and different modulations in the model parameters are considered for both linear and/or nonlinear terms. Specifically, identical periodic modulation of the model parameters for the positive and negative feedback is included in the first case, where it is observed that the Gompertz model does not forget its initial values as the system's response time is quite large than the disturbance's time-scale. That is, initial values far from equilibrium x^* can never reach the equilibrium point. In view of sustainability, a maximum Fisher information is noticed for $x_0 \simeq x^*$; Fisher information increases with x_0 up to $x_0 \simeq x^*$ and decreases beyond $x_0 \simeq x^*$. This behavior is due to the high variability in the model parameters beyond $x_0 \simeq x^*$; low variability (more sustainable) yields high Fisher information whereas high variability leads to low Fisher information.

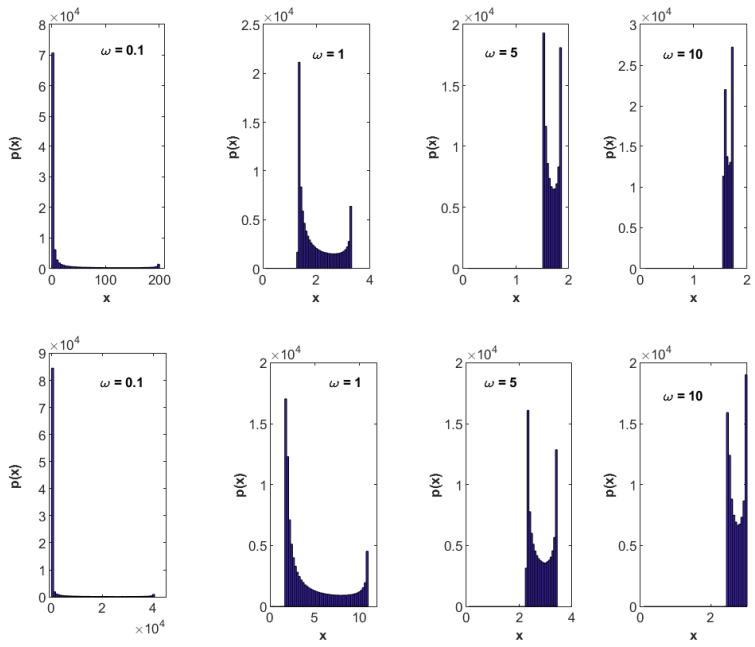

FIGURE 9. PDFs of x for two different $D_0 = 0.5$ and 1 in the upper and lower panels, respectively. For all cases, $x_0 = 0.1$, $B = 1$, and $c = 1$, PDFs are bimodal in all cases.

In the cases tested, the logistic and Gompertz models behave very similar in terms of information and sustainability although they evolve differently in time. It will be interesting to investigate different models using similar methods in the future.

REFERENCES

[1] A. AL-Saffar and E. Kim, *Sustainable theory of a logistic model-Fisher information approach*, Math. Biosciences, **285**(2017), 81–91.

[2] H. Cabezac, and B. D. Fath, *Towards a theory of sustainable systems*, Fluid Phase Equilibria, **194**(2002), 3–14.

[3] B. D. Fath, H. Cabezas, and Ch. W. Pawlowski, *Regime changes in ecological systems: an information theory approach*, J. Theor. Bio., **222**(2003), 517–530.

[4] D. Jukic, G. Kralik, and R. Scitovski, *Least-squares fitting Gompertz curve*, J. Computational and Applied Math., **169**(2004), 359–375.

[5] K. Kartono, P. Purwanto, and S. Suripin, *Ecological Implications of the Dynamics of Water Volume Growth in a Reservoir*, Ecological Engineering & Environmental Technology, **22**(2021), 22–29.

[6] E. Konig, Cabezas, H. and A. L. Mayer, *Detecting dynamic system regime boundaries with Fisher information: the case of ecosystems*, Clean Techn Environ Policy, **21**(2019), 1471–1483.

[7] A. K. Laird, *Dynamics of tumour growth*, Br. J. Cancer, **18**(1964), 490-502.

[8] A. K. Laird, *Dynamics of tumour growth: comparison of growth rates and extrapolation of growth curve to one cell*, Br. J. Cancer, **19**(1965), 278–291.

[9] A. L. Mayer, Ch. W. Pawlowski, and H. Cabezas, *Fisher Information and dynamic regime changes in ecological systems*, Ecological Modelling, **195**(2006), 72–82.

[10] A. G. Nobile, L. M. Ricciardi, and L. Sacerdote, *On Gompertz growth model and related difference equations*, Biol. Cybern., **42**(1982), 221–229.

[11] V. Rico-Ramirez, M. A. Reyes-Mendoza, P. A. Quintana-Hernandez, J. A. Ortiz-Cruz, S. Hernandez-Castro, and U. M. Diwekar *Fisher information on the performance of dynamic systems*, Ind. and Eng. Chem. Res., **49**(2010), 1812–1821.

[12] Sh. Tabassum, N. B. Rosli, and M. S. A. B. Mazalan, *Mathematical modeling of cancer growth process: a review*, In J. Phys.: Conference Series, **1366**(2019): 012018.

[13] L.M. Tenkes, R. Hollerbach, and E. Kim, *Time-dependent probability density functions and information geometry in stochastic logistic and Gompertz models*, J. Stat. Mech.: Theory and Experiment **12**(2017): 123201.

[14] P. Waliszewski, and J. Konarski, *The Gompertzian curve reveals fractal properties of tumor growth*, Chaos, Solitons and Fractals **16**(2003), 665–674.

[15] P. Waliszewski, *A principle of fractal-stochastic dualism and Gompertzian dynamics of growth and self-organization*, BioSystems **82**(2005), 61–73.

[16] Z. Wang, and M. Liu, *Optimal impulsive harvesting strategy of a stochastic Gompertz model in periodic environments*, App. Math. Letters **125**(2022): 107733.

[17] CH. P. Winsor, *The Gompertz curve as a growth curve*, Proceedings of the national academy of sciences **18**(1932), 1–8.

[18] M. H. Zwietering, I. Jongenburger, F. M. rombouts and K. Van't riet, *Modeling of the bacterial growth curve*, App. and Enviro. Microbiology, **56**(1990), 1875–1881.

Corresponding author, Department of Statistics, University of Duhok, Duhok, Iraq
Email address: avan.elias@uod.ac

Fluid and Complex Systems Center, Coventry University, Coventry, United Kingdom
Email address: E.Kim@shef.ac.uk